DRAL
Daresbury Laboratory
Rutherford Appleton Laboratory

RAL Report
RAL-95-035

Analytic Approach to Small x Structure Functions

J R Forshaw R G Roberts and R S Thorne

March 1995

Rutherford Appleton Laboratory Chilton DIDCOT Oxfordshire OX11 0QX

RAL-95-035
April 1995

Analytic Approach to Small x Structure Functions

J.R. Forshaw, R.G. Roberts and R.S.Thorne
Rutherford Appleton Laboratory,
Chilton, Didcot OX11 0QX, England.

Abstract

We present a method for the analytic solution of small x structure functions. The essential small x logarithms are summed to all orders in the anomalous dimensions and coefficient functions. Although we work at leading logarithmic accuracy, the method is general enough to allow the systematic inclusion of sub-leading logarithms. Results and predictions are presented for the gluon density, and the structure functions $F_2(x,Q^2)$ and $F_L(x,Q^2)$. We find that corrections to the simple double logarithmic calculation are important in the HERA range and obtain good fits to all available data.

As a result of the recent work of Catani and Hautmann [1], it is now possible to include the dominant small x dynamics encompassed by the formalism of Balitsky, Fadin, Kuraev and Lipatov (BFKL) [2] within the framework of the renormalisation group and collinear factorisation, and some (mostly numerical) studies have already been performed [3, 4]. In this paper, we wish to present an analytic solution to the relevant evolution equations and their convolution with the appropriate coefficient functions. Throughout we work in the high energy limit, i.e. we sum all terms in the perturbative expansion of the cross section which are

$$\sim \left(\alpha_s \ln \frac{s}{Q^2}\right)^n,$$

where s is the relevant centre-of-mass energy and Q^2 characterises the typical short distances involved. We shall focus on deep inelastic scattering at the DESY ep collider, HERA. In which case, $\sqrt{s}$ is the γp centre-of-mass energy and $-Q^2$ is the photon virtuality, i.e. the Bjorken-x variable, $x \approx Q^2/s$. Our approach is quite general and it will be clear how to extend it beyond the leading logarithmic accuracy.

Altarelli-Parisi Evolution at small x and the gluon density

Recall the Dokshitzer, Gribov, Lipatov, Altarelli, Parisi (DGLAP) equations for the parton distribution functions [5]:

$$\frac{\partial f_N^i(Q^2)}{\partial \ln Q^2} = \sum_j \gamma_N^{ij} f_N^j(Q^2). \tag{1}$$

$f_N^i(Q^2)$ is the Nth moment of the momentum distribution for partons of type i and γ_N^{ij} is the anomalous dimension matrix, i.e.

$$\begin{aligned} f_N^i(Q^2) &= \int_0^1 dx\, x^{N-1} f^i(x,Q^2), \\ \gamma_N^{ij} &= \int_0^1 dx\, x^N P_{ij}(x). \end{aligned} \tag{2}$$

Our notation is such that the important gluon anomalous dimension,

$$\gamma_N^{gg} = \frac{\bar{\alpha}_s}{N} + 2\zeta(3)\left(\frac{\bar{\alpha}_s}{N}\right)^4 + ... \tag{3}$$

and $\bar{\alpha}_s = 3\alpha_s/\pi$.

These equations are solved given the boundary conditions, $f_N^i(Q_0^2)$, i.e. they allow the Q^2-dependence of the parton distribution functions to be determined but not their absolute normalisation.

In the high energy (i.e. small x) limit, we keep only those terms in the anomalous dimension matrix which are $\sim (\alpha_s/N)^n$, i.e. the leading logarithmic terms in the splitting functions. In this case, evolution is driven by γ_N^{gg}, which satisfies [2, 6]

$$1 = \frac{\bar{\alpha}_s}{N}\chi(\gamma_N^{gg}), \tag{4}$$

where

$$\chi(\gamma) = 2\psi(1) - \psi(\gamma) - \psi(1-\gamma) \tag{5}$$

and $\psi(\gamma)$ is the Euler-gamma function. The first two non-zero terms in the series expansion are written in eq.(3). The DGLAP equations then have the simple solution:

$$\begin{aligned} f_N^s(Q^2) &= f_N^s(Q_0^2), \\ f_N^g(Q^2) &= \left[f_N^g(Q_0^2) + \frac{4}{9}f_N^s(Q_0^2)\right]\exp\left(\int_{Q_0^2}^{Q^2}\frac{dk^2}{k^2}\gamma_N^{gg}\right) - \frac{4}{9}f_N^s(Q_0^2). \end{aligned} \tag{6}$$

The singlet quark density is $f_N^s(Q^2) = \sum_i f_N^i(Q^2)$ where the sum runs over all quarks and anti-quarks. Since we work in the small x region, we expect the gluon density to be dominant and subsequently drop all reference to the singlet density (except implicitly in the input to $F_2(x,Q^2)$). We have explicitly checked that this makes very little quantitative difference to our results.

In order to construct a sensible gluon structure function, we do not merely invert the N-space solution above. It is more natural to define the gluon structure function to be that object which would be observed if we had a coloured current available as our probe. In which case there are important contributions which arise, not only from the QCD evolution but also from the coefficient function. One can think of such corrections as arising from graphs which should not be exponentiated via the renormalisation group and so contain no explicit strong ordering of the rung momenta. These graphs are essential for a sensible defintion of the gluon density (e.g. as the object which is closely related to the structure function $F_L(x,Q^2)$) and for consistency with the gluon density which is constructed by integrating the 'unintegrated gluon density', $\mathcal{F}(x,k^2)$, obtained by solving the BFKL equation. To see this, we start from the BFKL defintion of the gluon density, i.e.

$$G(x,Q^2) = \int_0^\infty \frac{dk^2}{k^2}\int_x^1 \frac{dz}{z}\delta(1-x/z)\Theta(Q^2-k^2)\mathcal{F}(z,k^2). \tag{7}$$

The hard scatter cross section which is to be convoluted with $\mathcal{F}(x,k^2)$ is thus

$$\hat{\sigma}_N(k^2/Q^2) = \int_0^1 dx x^{N-1}\delta(1-x)\Theta(Q^2-k^2). \tag{8}$$

Now, in the formalism of Catani and Hautmann[1],

$$G_N(Q^2) = \gamma_N^{gg} \int_0^\infty \frac{dk^2}{k^2} \left(\frac{k^2}{Q^2}\right)^{\gamma_N^{gg}} \hat{\sigma}_N(k^2/Q^2)\, R_N\, f_N^g(Q^2), \tag{9}$$

i.e.

$$G_N(Q^2) = R_N\, f_N^g(Q^2). \tag{10}$$

The important factor, R_N, is given by

$$\begin{aligned} R_N = \quad & \left\{\frac{\Gamma(1-\gamma_N^{gg})\,\chi(\gamma_N^{gg})}{\Gamma(1+\gamma_N^{gg})\,[-\gamma_N^{gg}\,\chi'(\gamma_N^{gg})]}\right\}^{1/2} \times \\ & \exp\left\{\gamma_N^{gg}\psi(1) + \int_0^{\gamma_N^{gg}} d\gamma \frac{\psi'(\gamma) - \psi'(1-\gamma)}{\chi(\gamma)}\right\}. \end{aligned} \tag{11}$$

Solution in x-space

Let us now show how to invert the solution for $G_N(Q^2)$ back into x-space. We must perform the integral

$$G(x,Q^2) = \frac{1}{2\pi i}\int dN\, f_N^g(Q_0^2)\, R_N\, \exp\left(N\ln 1/x + Z_N(Q^2)\right) \tag{12}$$

where the integral is over a contour to the right of all singlarities, and

$$\begin{aligned} Z_N(Q^2) &= \int_{Q_0^2}^{Q^2} \frac{dk^2}{k^2}\gamma_N^{gg} \\ &= \frac{\gamma^2\zeta}{N} + \sum_{m=2}^{\infty} \frac{a_m}{m-1}\frac{\gamma^2}{N}\left[\left(\frac{\bar{\alpha}_s(Q_0^2)}{N}\right)^{m-1} - \left(\frac{\bar{\alpha}_s(Q^2)}{N}\right)^{m-1}\right] \\ &= \sum_{m=1}^{\infty} \frac{b_m(\zeta)}{N^m}. \end{aligned} \tag{13}$$

$\zeta = \ln(\alpha_s(Q_0^2)/\alpha_s(Q^2))$, $\gamma^2 = 12/\beta_0$ and, for consistency with the standard approach, we run the coupling at the scale k^2 (in the anomalous dimension integral). However, we note that at the leading logarithmic accuracy this is an essentially free choice. The coefficients a_n define the series expansion of the gluon anomalous dimension:

$$\gamma_N^{gg} = \sum_{n=1}^{\infty} a_n \left(\frac{\bar{\alpha}_s}{N}\right)^n. \tag{14}$$

We write the factor R_N also as a series expansion:

$$R_N = \sum_{n=0}^{\infty} c_n \left(\frac{1}{N}\right)^n, \tag{15}$$

and we note that $R_N = 1 + \frac{8}{3}\zeta(3)(\bar{\alpha}_s/N)^3 + ...$

We choose the boundary condition,

$$f_N^g(x, Q_0^2) = \mathcal{N}\Theta(x_0 - x),$$

which becomes $f_N^g(Q_0^2) = \mathcal{N}/N$ in moment space if we choose x/x_0 as the conjugate variable to N. This starting distribution is a good approximation to the expected $\sim (1-x)^5$ behaviour if $x_0 \sim 0.1$, and leads to reliable results for $x \lesssim 0.01$. The choice of a flat starting distribution (at small x) is motivated by the known behaviour of total cross sections at high energies, i.e. the 'soft' pomeron is known to have intercept close to 1 [7]. It is the small x behaviour one would expect in the absence of any perturbative QCD corrections.

We can now perform the N-plane integral by making the particular choice of contour to be the line from $r - i\infty$ to $r + i\infty$ plus a circle with centre at the origin and radius $r > 4\bar{\alpha}_s(Q_0^2)\ln 2$ (to ensure the analyticity of the integrand along the contour [4]). The value of the integral is now equal to that over the circle, and putting $N = re^{i\theta}$ we obtain in a straightforward manner:

$$\begin{aligned} G(x,Q^2) &= \mathcal{N}\sum_{i=0}^{\infty} c_i \left(\frac{\xi}{\gamma^2\zeta}\right)^{i/2} I_i(2\gamma\sqrt{\xi\zeta}) \\ &+ \mathcal{N}\sum_{i=0}^{\infty}\sum_{j=2}^{\infty} c_i b_j \left(\frac{\xi}{\gamma^2\zeta}\right)^{(i+j)/2} I_{i+j}(2\gamma\sqrt{\xi\zeta}) \\ &+ \mathcal{N}\sum_{i=0}^{\infty}\sum_{j=2}^{\infty}\sum_{k=2}^{\infty} \frac{c_i b_j b_k}{2} \left(\frac{\xi}{\gamma^2\zeta}\right)^{(i+j+k)/2} I_{i+j+k}(2\gamma\sqrt{\xi\zeta}) + ... \end{aligned} \tag{16}$$

where $\xi = \ln(x_0/x)$. We note that exactly the same method could be used if we were to choose a powerlike input, or even the $(1-x)^5$ behaviour. One simply finds the moment space expression for the input and expands in powers of N. We also note that for small x the result obtained using the saddle-point method to evaluate eq.(12) does not give a good approximation and provides misleading results. This failure occurs essentially because, along the contour of steepest decent, the integrand does not fall quickly enough for values of N far from the saddle-point.

Let us now discuss our solution. Firstly, we see explicitly the double log result,

$$G(x, Q^2) \sim I_0(2\gamma\sqrt{\xi\zeta}),$$

which arises when only the leading order (in α_s) terms are kept. Going beyond this first term, the inverse factorials associated with the Bessel functions ensure that the summations in our expression converge for all x, despite the fact that the expansions of γ_N^{gg} and R_N diverge for

$N < 4\bar{\alpha}_s \ln 2$. This effect of convergence in x-space was pointed out using a similar, but slightly less direct, argument in [3]. Using the first sum in eq.(16) we can recover the power behaviour of the structure function at small enough x. It arises after taking the small argument expansion of the Bessel function (which is appropriate for large order Bessel functions) and using the fact that $c_{n+1}/c_n = 4\bar{\alpha}_s \ln 2$ for asymptotically large n, i.e. the general term in the sum over i is

$$\sim (4\bar{\alpha}_s \ln 2)^i \left(\frac{\xi}{\gamma^2 \zeta}\right)^{i/2} \frac{(\gamma^2 \zeta \xi)^{i/2}}{i!} = \frac{(4\xi\bar{\alpha}_s \ln 2)^i}{i!}.$$

A similar power behaviour is generated by the other terms in eq.(16), i.e. due to the Q^2-evolution, but they are not important for all practical values of x. The same qualitative conclusion has been reached in ref.[3], where a sum of Bessel functions was presented as an approximate solution for $f^g(x, Q^2)$. In other words, the dominant corrections to the double log result are due to the presence of the R_N factor, i.e. the corrections to the evolution are small (due to the relatively small size of the coefficients in the expansion of the gluon anomalous dimension), only becoming dominant at very large Q^2 and/or very small x. Up to logarithms in Q^2 (which arise due to the running of the coupling in R_N), one can interpret $R_N f_N^g(Q_0^2)$ as the input gluon distribution, i.e. the BFKL corrections essentially 'renormalise' the starting gluon density.

The fraction of $G(x, Q^2)$ which arises solely from the double log graphs (i.e. the I_0 Bessel function) is presented in the contour plot shown in fig.(1). It can be seen that the high energy (BFKL) corrections are significant over the HERA range despite the fact that the coefficients c_1 and c_2 vanish. We note that the contribution from the BFKL corrections to the evolution (i.e. those terms involving the b_i coefficients) are almost entirely negligible, in fact they contribute less than 4% over the x-Q^2 range probed at HERA. In fig.(2), we show the x dependence of $G(x, Q^2)$ at different Q^2 values and compare to the double log contribution. In all of our plots, we choose $x_0 = 0.1$ and take $\mathcal{N} = 1.1$ and $Q_0^2 = 2.0$. $\mathcal{N}$ and Q_0^2 are the only parameters for the gluon, and are fixed by fitting $F_2(x, Q^2)$ to the HERA data (see the following section for a discussion of this procedure). Note that our approach does not permit a flat gluon structure function, even though our input density was flat. This is in keeping with the standard BFKL result developed by direct solution of the BFKL equation. The scale Q_0 is to be understood as the scale below which we cannot use the perturbative approach. As such, we are unable to make any definite statements regarding the eventual saturation and flattening off of the small x structure functions (as Q^2 falls below Q_0^2) since this procedure is governed by physics beyond

that which is considered here. (However, we do see a hint of the breakdown of our approach, as we will discuss in the next section.) Indeed, we shall find that the quality of our fits to $F_2(x,Q^2)$ is largely insensitive to the choice of Q_0^2 once it is above ≈ 1 GeV^2. Our approach should be contrasted to that which attempts to evolve from some, typically quite low, value of Q_0^2 with a flat (or valencelike) starting distribution to higher Q^2 [8, 9].

Deep inelastic structure functions

In the previous section we concentrated on the gluon structure function, $G(x,Q^2)$. It involves no new techniques to extend the formalism to the case of the deep inelastic structure functions, $F_2(x,Q^2)$ and $F_L(x,Q^2)$. Eq.(10), which defines the gluon structure function, is merely a specific form of the more general expression for the dimensionless cross section, $F(x,Q^2)$:

$$F_N(Q^2) = C_N(Q^2/\mu_F^2) f_N^g(\mu_F^2) \tag{17}$$

where μ_F^2 is the factorisation scale (chosen to equal Q^2) and $C_N(Q^2/\mu_F^2)$ is the coefficient function (equal to R_N in the case of the gluon structure function).

Catani and Hautmann have shown that the coefficient function can be factorised into a product of the process independent (but factorisation scheme dependent) factor, R_N, and a process dependent factor, $h_N(\gamma_N^{gg})$, where [1]

$$h_N(\gamma) \equiv \gamma \int_0^\infty \frac{dk^2}{k^2} \left(\frac{k^2}{\mu_F^2}\right)^\gamma \hat{\sigma}_N(k^2/Q^2). \tag{18}$$

The hard subprocess cross section, $\hat{\sigma}_N(k^2/Q^2)$, is the lowest order (in α_s) cross section for scattering off-shell gluons (off the virtual photon in the case of deep inelastic scattering).

Thus, for the structure function, $F_L(x,Q^2)$

$$F_{L,N}(Q^2) = \langle e_q^2 \rangle h_{L,N}(\gamma_N^{gg})\, R_N\, f_N^g(Q^2) \tag{19}$$

with

$$h_{L,N}(\gamma) = \frac{\alpha_s}{2\pi} N_f T_R \frac{4(1-\gamma)}{3-2\gamma} \frac{\Gamma^3(1-\gamma)\Gamma^3(1+\gamma)}{\Gamma(2-2\gamma)\Gamma(2+2\gamma)} \tag{20}$$

and where $\langle e_q^2 \rangle$ is the mean quark charge squared. So, in order to evaluate $F_L(x,Q^2)$, we merely replace the c_n coefficients in eq.(16) by the corresponding coefficients in the expansion of $h_{L,N}(\gamma_N^{gg})\, R_N$.

Similarly,

$$h_{2,N}(\gamma) = \frac{2+3\gamma-3\gamma^2}{2(1-\gamma)} h_{L,N} \tag{21}$$

determines the Q^2-dependence of $F_2(x,Q^2)$, i.e.

$$\begin{aligned} \frac{\partial F_{2,N}(Q^2)}{\partial \ln Q^2} &= \langle e_q^2 \rangle (C^{(1)}_{g,N}(\alpha_s(Q^2)\gamma_N^{gg} + 2n_f\gamma_N^{qg}) f_N^g(q^2) \\ &= \langle e_q^2 \rangle \, h_{2,N}(\gamma_N^{gg}) \, R_N \, f_N^g(Q^2), \end{aligned} \tag{22}$$

to formally leading order.

In fig.(3), using the same choice of parameters (no more are needed) as in the discussion of $G(x,Q^2)$ previously, we present our predictions for the longitudinal structure function, $F_L(x,Q^2)$. As well as the full solution, we show the double log contribution. The largeness of the corrections to the double log calculation (in comparison to case of $G(x,Q^2)$), can be traced back to the fact that the second and third coefficients in the expansion of $h_{L,N}R_N$ are no longer zero. Also shown in fig.(3) is the result of re-fitting the HERA data on $F_2(x,Q^2)$, while keeping only the double log Bessel function. In order unambiguously to establish the existence of the high energy corrections, it is ultimately necessary to expose deviations from the double log approach (or more precisely approaches which do not sum the infinity of high order corrections $\mathcal{O}(\alpha_s/N)$) and so this is the reason for our comparison. As seen, the prediction from the double log approach is mostly larger than that for the full expression, but flatter with x. This largeness comes about mainly because the starting scale is much lower, and hence there has been more time for evolution to take place.

Let us now turn to the structure function, $F_2(x,Q^2)$ and its comparison with the HERA data [10]. We start by considering the expression of eq.(22). In order to construct $F_2(x,Q^2)$, we must integrate over Q^2 and invoke an input distribution, $F_2(x,Q_0^2)$. We choose this to be of the form $A + Bx^{-\lambda}$. We see no reason to believe that the input form of $F_2(x,Q^2)$ should be purely flat since, as demonstrated, the gluon structure function always has some powerlike behaviour due to the coefficient function. Indeed, we are not able to obtain a very good fit with a completely flat input. We could simply choose $Bx^{-\lambda}$, and are indeed able to obtain a comparable fit with such an input. However, our aim is not simply to obtain the best fit with the least number of parameters, but to determine the behaviour of the structure function as accurately as possible, and we believe the chosen input is the best way to do this. This introduces three extra parameters. The values of our 5 parameters (Q_0, the normalisation of the input gluon density and the three parameters in $F_2(x,Q_0^2)$) are then obtained by fitting to

the HERA data. Throughout, we work with 4 quark flavours and $\Lambda_{QCD} = 115$ MeV. Agreement with the data is very good, i.e. $\chi^2 = 48$ for the 92 data points which have $x < 0.01$.

Although we obtain very good agreement with the available HERA data, we expect our results to be subject to important corrections. Let us now explain why. In the leading log approximation, the structure function $F_2(x, Q^2)$ can be written in the form

$$\begin{aligned} F_{2,N}(Q^2) &= \langle e_q^2 \rangle C_{g,N}^{(1)}(\alpha_s(Q^2)) f_N^g(Q^2) + (C_{q,N}^{(0)} + C_{q,N}^{(1)}(\alpha_s(Q^2)) \sum_{i=1}^{2n_f} e_i^2 f_N^i(Q_0^2) \\ &+ 2n_f \langle e_q^2 \rangle C_{q,N}^{(0)}(\alpha_s(Q^2)) \int_{Q_0^2}^{Q^2} \frac{dq^2}{q^2} \gamma_N^{qg} f_N^g(q^2). \end{aligned} \tag{23}$$

The superscript on the coefficient functions specifies the order (in α_s) of the contribution, i.e. $C_{i,N} = \sum_n C_{i,N}^{(n)}$. At the Born level, $C_{g,N}^{(0)} = 0$ and $C_{q,N}^{(0)} = 1$.

Taking the derivative of this expression leads to eq.(22), but only after neglecting the higher order terms which are induced by differentating the coefficient functions. Such terms are formally sub-leading since

$$\frac{\partial}{\partial \ln Q^2} = -\alpha_s^2 \frac{\beta_0}{4\pi} \frac{\partial}{\partial \alpha_s}.$$

However, they are not sub-leading once eq.(22) is integrated to form the structure function, $F_2(x, Q^2)$.

To see how important these corrections are expected to be, we expand the coefficient function

$$C_{g,N}^{(1)} = \sum_{n=0}^{\infty} p_n \, \bar{\alpha}_s \left(\frac{\bar{\alpha}_s}{N} \right)^n. \tag{24}$$

The ratio of the term $\sim \bar{\alpha}_s(\bar{\alpha}_s/N)^m$ in $\partial C_{g,N}^{(1)}/\ln Q^2$ to the corresponding term in the series expansion of $C_{g,N}^{(1)} \, \gamma_N^{gg}$ is thus

$$\left(-\frac{\beta_0 \alpha_s}{4\pi} \right) \frac{(m+1)\, b_m}{\sum_{i=0}^{m-1} b_{i+1} a_{m-i}}. \tag{25}$$

Since $a_{n+1}/a_n = 4 \ln 2$ for large n and, assuming a similar relation for the p_n coefficients, it follows that this ratio becomes

$$\sim -\frac{\beta_0 \alpha_s}{4\pi} \frac{1}{A}$$

where $a_n \approx A \, (4 \ln 2)^{n-1}$. Since $A \ll 1$ we cannot ignore such contributions. We should emphasise that p_{n+1}/p_n cannot exceed $4 \ln 2$ (since we know the dominant singularity arises at $N = 4\bar{\alpha}_s \ln 2$) and that assuming any $p_{n+1}/p_n < 4 \ln 2$ leads to an even stronger enhancement of the derivative terms (e.g. by a factor of m for $p_{n+1}/p_n \ll 4 \ln 2$). All the evidence from the

calculation of the series expansion of the coefficient function is that p_{n+1}/p_n is indeed $\sim 4\ln 2$ for large n.

Although these corrections are formally sub-leading, we believe it is unlikely that they will cancel with higher order graphs and as such it is safe (and indeed more appropriate) to include them in this order of the calculation. Since they lead to a negative contribution to $\partial F_2(x,Q^2)/\partial \ln Q^2$, we therefore expect a reduction in $\partial F_2(x,Q^2)/\partial \ln Q^2$ as x falls at fixed Q^2 (or Q^2 falls at fixed and small x).

We have computed the series expansions of the gluon coefficient function, $C^{(1)}_{g,N}$, and the anomalous dimension, γ^{qg}_N, in the $\overline{\rm MS}$ scheme to 18th order (we will shortly have more to say on the choice of scheme). As mentioned, we neglect the $\mathcal{O}(\alpha_s)$ contribution to the quark coefficient function (since the input quark density is small in comparison to the evolved gluon density and the quark coefficient function is smaller than that for the gluon). As a result, we are able to compute $F_2(x,Q^2)$ including those corrections which were neglected when eq.(22) was integrated over Q^2. The solid line in fig.(4) shows the result of a new fit to the HERA data and improvement in the χ^2 of the fit is found, i.e. $\chi^2 = 45$ for the 92 data points. A considerable improvement in the insensitivity to the value of Q^2_0 is also found. For our best fit $Q^2_0 = 2.0$ and $\mathcal{N} = 1.1$, and these are the parameters used to determine our predictions for $G(x,Q^2)$ and $F_L(x,Q^2)$. We also find the input to $F_2(x,Q^2)$ to be $0.15 + 0.035x^{-0.4}$.

From our results we conclude that our choice of a Θ-function form of the gluon input is appropriate. Also, it is significant that the χ^2 only significantly worsens once $Q^2_0 \lesssim 1$ GeV^2. This is consistent with idea that the scale at which we define our input should be essentially arbitrary, providing it is large enough for the perturbative expansion to apply, and not too large to fill the available phase space. The dotted line in the figure shows the previously discussed best fit for $F_2(x,Q^2)$, i.e. ignoring the derivatives of the coefficient function. The dashed line shows the best fit taking only the leading term in the Bessel function expansion, i.e. the double log result, and flat inputs for the gluon and for $F_2(x,Q^2)$. This also has a very good χ^2 of 44 for the 92 points, but high sensitivity to Q^2_0. It is clear from the plots that the differences between the full leading log calculation of $F_2(x,Q^2)$ and the dotted (and dashed) line are consistent with our expectations. In particular, from the lowest Q^2 and lowest x bins of the H1 data, we tentatively suggest that our predicition of a flatter (in Q^2) $F_2(x,Q^2)$ is quite possibly supported by the data.

As a slight word of caution we must note that for low enough x, $\partial F_2(x,Q^2)/\partial \ln Q^2$ even-

tually becomes negative, and $F_2(x,Q^2)$ rises for falling Q^2. It is this region of negative $\ln Q^2$ derivative where our calculation starts to become untrustworthy. However, the effect only sets in for $x \sim 10^{-4}$ at $Q^2 = Q_0^2$, and the value of x at which $\partial F_2(x,Q^2)/\partial \ln Q^2 = 0$ falls very rapidly as Q^2 increases. Similarly, we feel that the predictions for the gluon and $F_L(x,Q^2)$ should be viewed with a little caution at extremely low x and small Q^2 . Nevertheless, it is reassuring that the region of breakdown is where we would expect physics beyond that considered in our approach to become important.

It is also important to comment on our choice of scheme. We could just as well have computed $F_2(x,Q^2)$ in the DIS scheme (and obtained precisely the same results as in $\overline{\rm MS}$). This is true providing we take care to include the sub-leading corrections to γ_N^{qg} which contribute in the leading order to $F_2(x,Q^2)$. These terms are those neglected in eq.(5.27) of Catani and Hautmann when transforming to DIS scheme.

It has recently been suggested that higher order corrections in the evolution may well be very important, i.e. due to the exponentiation of the γ_N^{qg} anomalous dimension. We suggest that this may not be the case. The conclusions of Ellis *et al* [4] are based upon the fact that, in the DIS scheme, the coefficients of the $\alpha_s \mathcal{O}(\alpha_s/N)$ contributions to γ_N^{qg} are large (in comparison to the corresponding coefficients in the leading order expansion of γ_N^{gg}). At the leading order, γ_N^{qg} occurs only in the 'coefficient function' of $\partial F_{2,N}(Q^2)/\partial \ln Q^2$. Indeed in the DIS scheme it completely determines the 'coefficient function', i.e.

$$2n_f\, \gamma_N^{qg} = R_N\, h_{2,N}(\gamma_N^{gg}), \tag{26}$$

(where we should, of course, also include the terms from the derivative of the $\overline{\rm MS}$ coefficient function). Now, if we interpret the factor R_N as before, i.e. not to be associated with the renormalisation group exponentiation, then we anticipate two things. Firstly, in the $\overline{\rm MS}$ scheme, the coefficients of γ_{qg} should be much smaller than the corresponding ones in the DIS scheme. Indeed we find this to be so: the corresponding terms differing by an order of magnitude at large orders. Secondly, in a complete next to leading order calculation using the DIS scheme there should be large cancellations which reduce the impact of the large γ_N^{qg} as calculated in the DIS scheme. Since this higher order calculation relies upon higher order corrections to γ_N^{gg} as far as the evolution is concerned, and on the coefficients of the $\alpha_s^2 \mathcal{O}(\alpha_s/N)$ expansion of γ_N^{qg} for the 'coefficient function', neither of which has yet been evaluated, we believe it is premature to draw such strong conclusions regarding the role of sub-leading corrections in the evolution of the parton densities.

Conclusions

We have presented an analytic approach to the evaluation of small x cross sections and studied the behaviour of the gluon structure function, defined in a way which is consistent with the previous studies based upon the direct solution to the BFKL equation. In particular the solution in x-space is obtained exactly, and explicitly reveals the extreme limits of the double leading log result and the power behaviour expected from the BFKL approach. In addition, we examined the deep inelastic structure functions $F_2(x,Q^2)$ and $F_L(x,Q^2)$ and demonstrated that the high energy corrections (to the double log calculation) are significant in the HERA region. Consistency with the data on $F_2(x,Q^2)$ is found. The structure function $F_L(x,Q^2)$ and the Q^2 dependence of $F_2(x,Q^2)$ should be able to provide sensitive tests of the small x dynamics; in particular deviations from the traditional approach (expansion in α_s) may well be observable.

We have not discussed the process of heavy quark production (in deep inelastic scattering or in photoproduction), although this process also ought to shed important light on the essential dynamics [11]. Also, the recent measurement by the ZEUS collaboration of the dijet cross section in photoproduction [12] could be confronted with theory using the techniques presented here [13]. Finally, we wish to make available the expansion (in α_s/N) of the coefficient function, R_N, and the $\overline{\rm MS}$ scheme expansions of the quark anomalous dimension γ_N^{qg} and the gluon coefficient function $C_{g,N}^{(1)}$. These are displayed in the following table.

Acknowledgments

We wish to thank Keith Ellis, Francesco Hautmann and Graham Ross for helpful discussion.

Table

Values of the first 18 coefficients in series expansions:

$$\gamma_N^{qg(\overline{\rm MS})} = \frac{\alpha_s}{2\pi}\frac{1}{3}\sum_{n=0}^{\infty} a_n^{qg}\left(\frac{\bar{\alpha}_s}{N}\right)^n,$$

$$C_{g,N}^{(1)(\overline{\rm MS})} = \frac{\alpha_s}{2\pi} n_f \frac{1}{3}\sum_{n=0}^{\infty} \tilde{p}_n\left(\frac{\bar{\alpha}_s}{N}\right)^n,$$

$$R_N^{(\overline{\rm MS})} = \sum_{n=0}^{\infty} \tilde{c}_n\left(\frac{\bar{\alpha}_s}{N}\right)^n,$$

i.e. $\tilde{p}_n = \frac{n_f}{18} p_n$ (see eqn.(24)) and $\tilde{c}_n \bar{\alpha_s}^n = c_n$ (see eqn.(15)).

n	a_n^{qg}	$\tilde{p}_n$	$\tilde{c}_n$
0	1.00	1.00	1.00
1	1.67	1.49	0.00
2	1.56	9.71	0.00
3	3.42	1.64×10^{1}	3.21
4	5.51	3.91×10^{1}	-0.811
5	7.88	1.29×10^{2}	4.56
6	2.57×10^{1}	2.41×10^{2}	3.27×10^{1}
7	4.42×10^{1}	6.53×10^{2}	-2.95
8	8.77×10^{1}	1.93×10^{3}	1.08×10^{2}
9	2.83×10^{2}	4.01×10^{3}	4.00×10^{2}
10	5.11×10^{2}	1.14×10^{4}	1.33×10^{2}
11	1.24×10^{3}	3.17×10^{4}	2.10×10^{3}
12	3.68×10^{3}	7.18×10^{4}	5.51×10^{3}
13	7.17×10^{3}	2.07×10^{5}	5.30×10^{3}
14	1.91×10^{4}	5.52×10^{5}	3.85×10^{4}
15	5.29×10^{4}	1.33×10^{6}	8.49×10^{4}
16	1.12×10^{5}	3.82×10^{6}	1.40×10^{5}
17	3.11×10^{5}	1.00×10^{7}	6.95×10^{5}

References

[1] S. Catani, F.Fiorani, G. Marchesini and G. Oriani, Nucl. Phys. **B361** (1991) 645;

S. Catani, M. Ciafaloni and F. Hautmann, Phys. Lett. **B242** (1990) 97; Nucl. Phys. **B366** (1991) 135; Phys. Lett. **B307** (1993) 147;

S. Catani and F. Hautmann, Phys. Lett. **B315** (1993) 157; Nucl. Phys. **B427** (1994) 475.

[2] L.N. Lipatov, Sov. J. Nucl. Phys. **23** (1976) 338;

V.S. Fadin, E.A. Kureav and L.N. Lipatov, Phys. Lett. **B60** (1975) 50; Sov. Phys. JETP **44** (1976) 443; Sov. Phys. JETP **45** (1977) 199;

Y.Y. Balitski and L.N. Lipatov, Sov. J. Nucl. Phys. **28** (1978) 822.

[3] R.D. Ball and S. Forte, CERN Preprint - Th/95-1, January 1995.

[4] R.K. Ellis, F. Hautmann and B.R. Webber, Cavendish preprint - HEP - 94/18.

[5] V.N. Gribov and L.N. Lipatov, Sov. J. Nucl. Phys. **15** (1972) 438;

L.N. Lipatov, Sov. J. Nucl. Phys. **20** (1974) 94;

G. Altarelli and G. Parisi, Nucl. Phys. **B126** (1977) 298.

[6] T. Jaroszewicz, Phys. Lett. **B116** (1982) 291.

[7] P.D.B. Collins and F. Gault, Phys. Lett. **B112** (1982) 255;

A. Donnachie and P.V. Landshoff, Nucl. Phys. **B244** (1984) 322; Nucl. Phys. **B267** (1986) 690.

[8] M. Glück, E. Reya and A. Vogt, Phys. Lett. **B306** (1993) 391.

[9] R.D.Ball and S.Forte, Phys. Lett. **B335** (1994) 77; Phys. Lett. **B336** (1994) 77.

[10] ZEUS collaboration: M. Derrick *et al*, DESY preprint 94-143 (1994);

H1 collaboration: T. Ahmed *et al*, DESY preprint, 95-006 (1995).

[11] S. Catani, M. Ciafaloni and F. Hautmann, Nucl. Phys. **B366** (1991) 135.

[12] ZEUS collaboration: M. Derrick *et al*, DESY preprint 95-033, 1995.

[13] J.R. Forshaw and R.G. Roberts, Phys. Lett. **B319** (1993) 539; Phys. Lett. **B335** (1994) 494.

Figure Captions

[1] Contour plot exhibiting the contribution to the full gluon structure function made by the double leading log term.

[2] Gluon structure function $G(x, Q^2)$ as a function of x plotted for a range of Q^2 values. Contribution made by double leading log approximation shown by dot-dashed line.

[3] Prediction of longitudinal structure function $F_L(x, Q^2)$ as a function of x plotted for a variety of Q^2 values. Contribution made by double leading log term shown by dot-dashed line. Also shown by dashed line is the prediction made using the best fit for $F_2(x, Q^2)$ while keeping only the double log term.

[4] Comparison of theoretical predictions with the small x (i.e. $x < 0.005$) data from the (a) ZEUS collaboration (renormalised up 2%) and the (b) H1 collaboration (renormalised down 4%). The dotted line corresponds to the best fit for this expression minus the formally subleading terms coming from the derivative of the coefficient function and the dashed line to the best fit for the double leading log approximation.

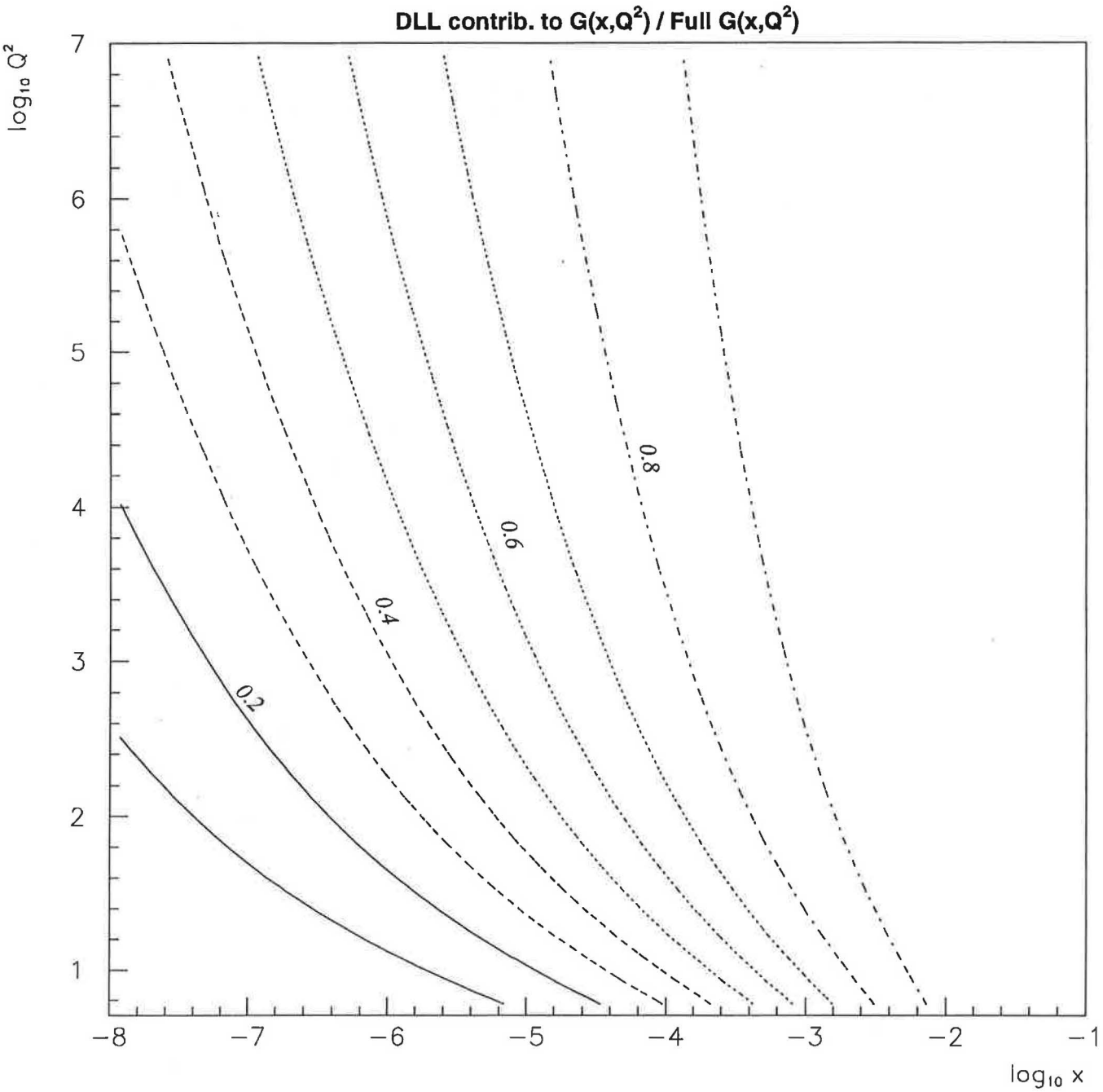
DLL contrib. to G(x,Q²) / Full G(x,Q²)
log₁₀ Q²
7
6
5
4
3
2
1
0.2
0.4
0.6
0.8
−8
−7
−6
−5
−4
−3
−2
−1
log₁₀ x

Fig. 1

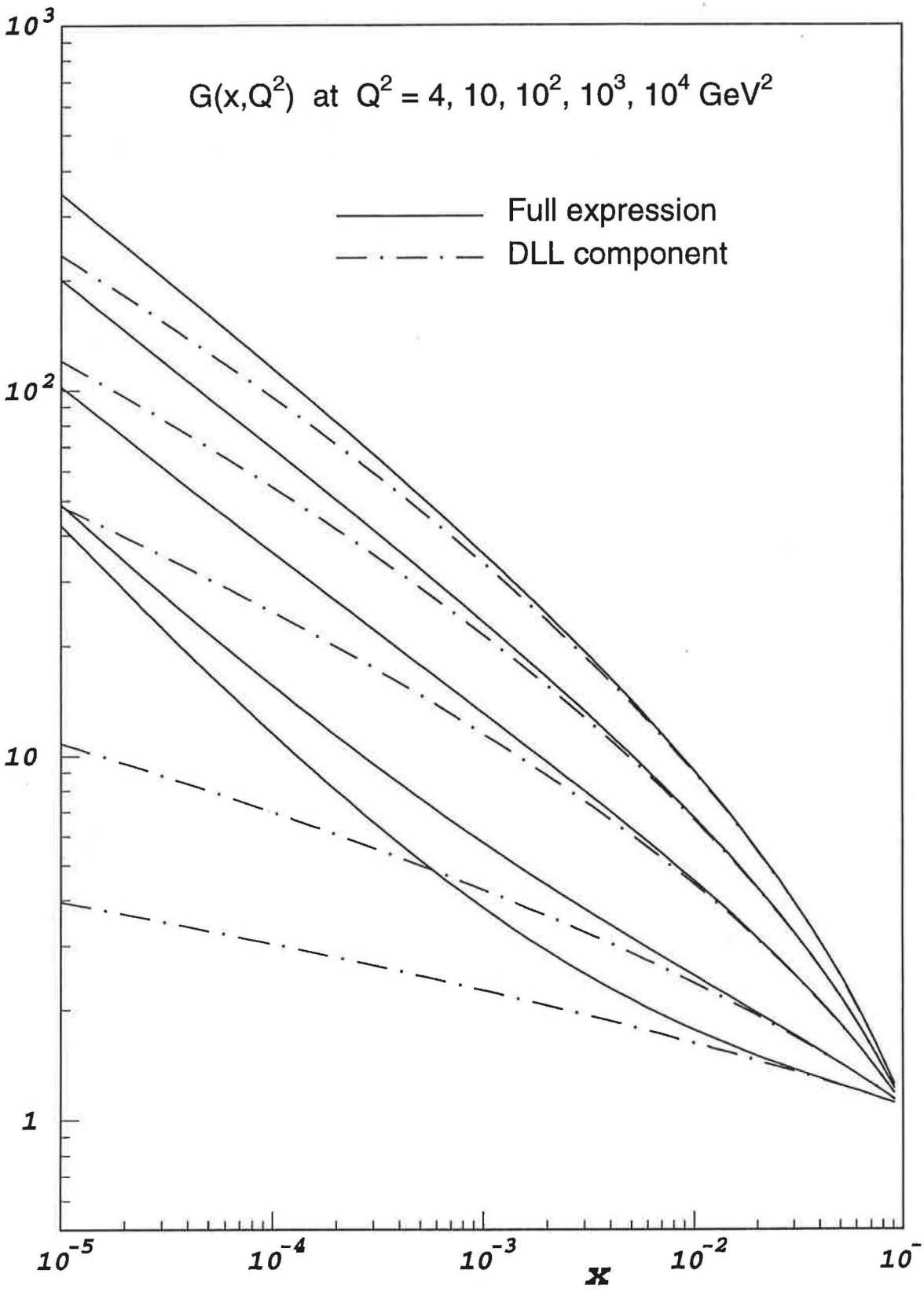
10^3
10^2
10
1
$G(x,Q^2)$ at Q^2 = 4, 10, 10^2, 10^3, 10^4 GeV^2
Full expression
DLL component
10^{-5}
10^{-4}
10^{-3}
10^{-2}
10^{-1}
x

Fig. 2

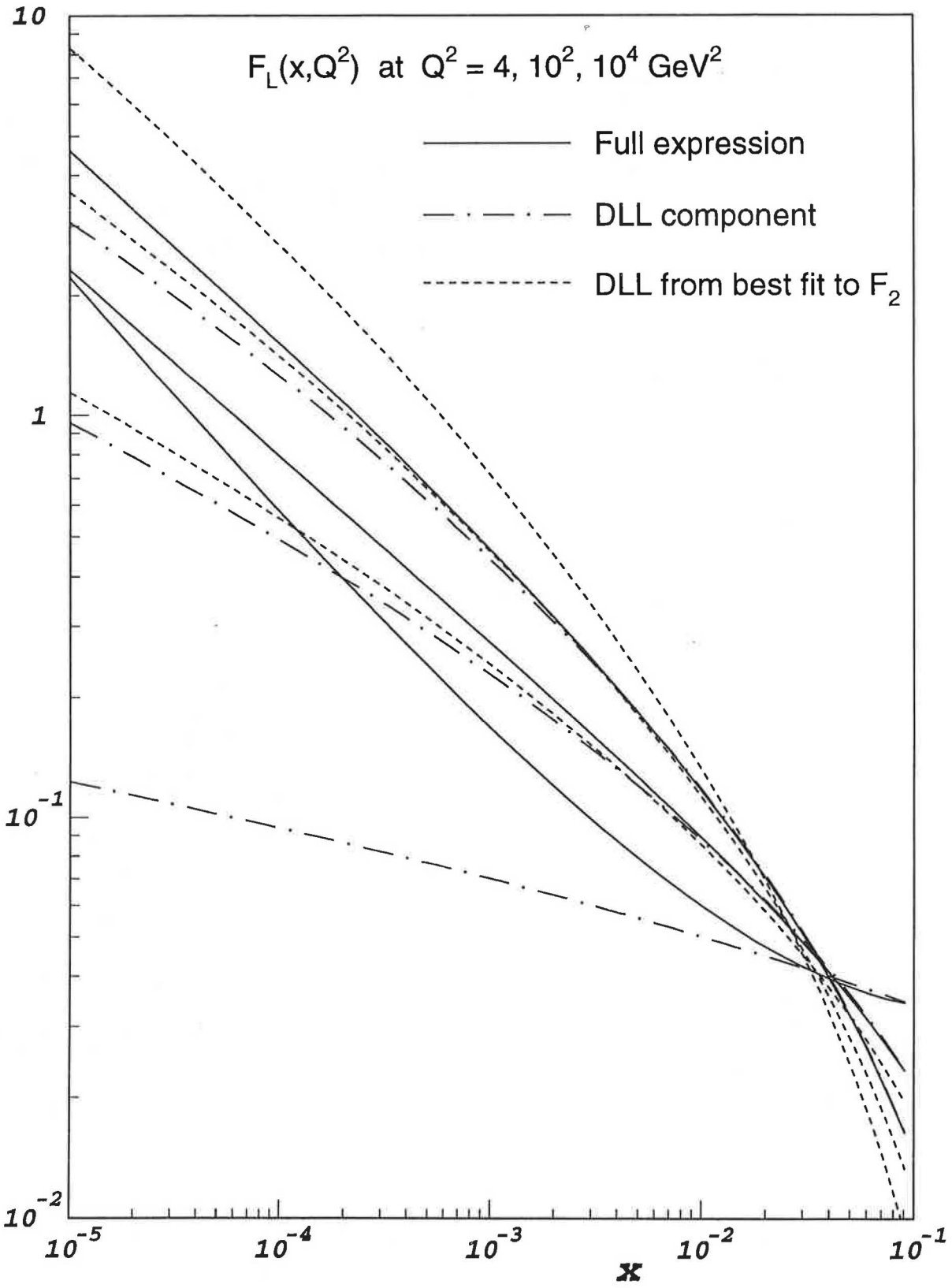
10
1
10^{-1}
10^{-2}
$F_L(x,Q^2)$ at $Q^2 = 4, 10^2, 10^4$ GeV^2
Full expression
DLL component
DLL from best fit to F_2
10^{-5}
10^{-4}
10^{-3}
10^{-2}
10^{-1}
x

Fig. 3

H1(x0.96) comparison at small x

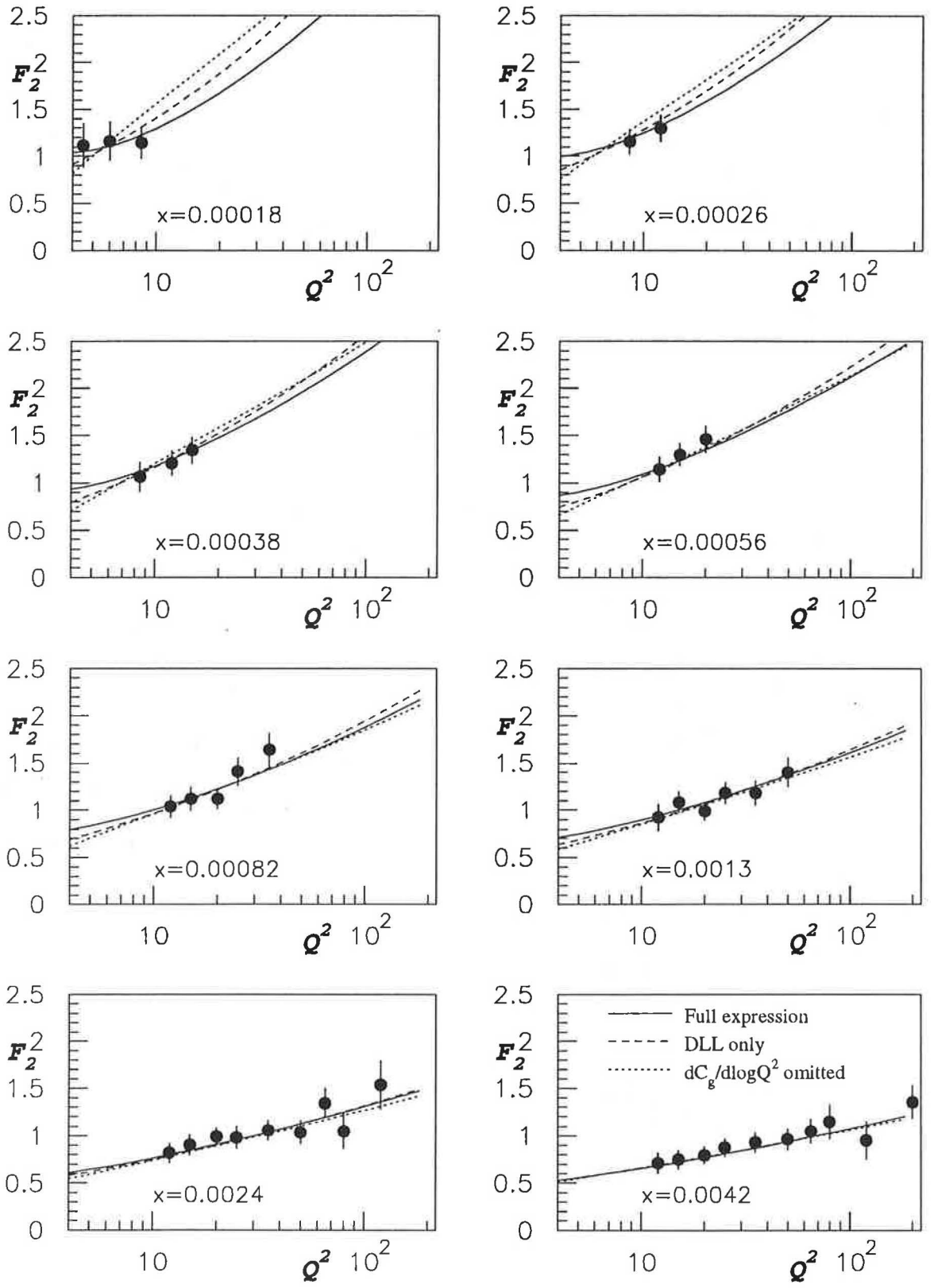

Fig. 4(a)

Zeus (x1.02) comparison at small x

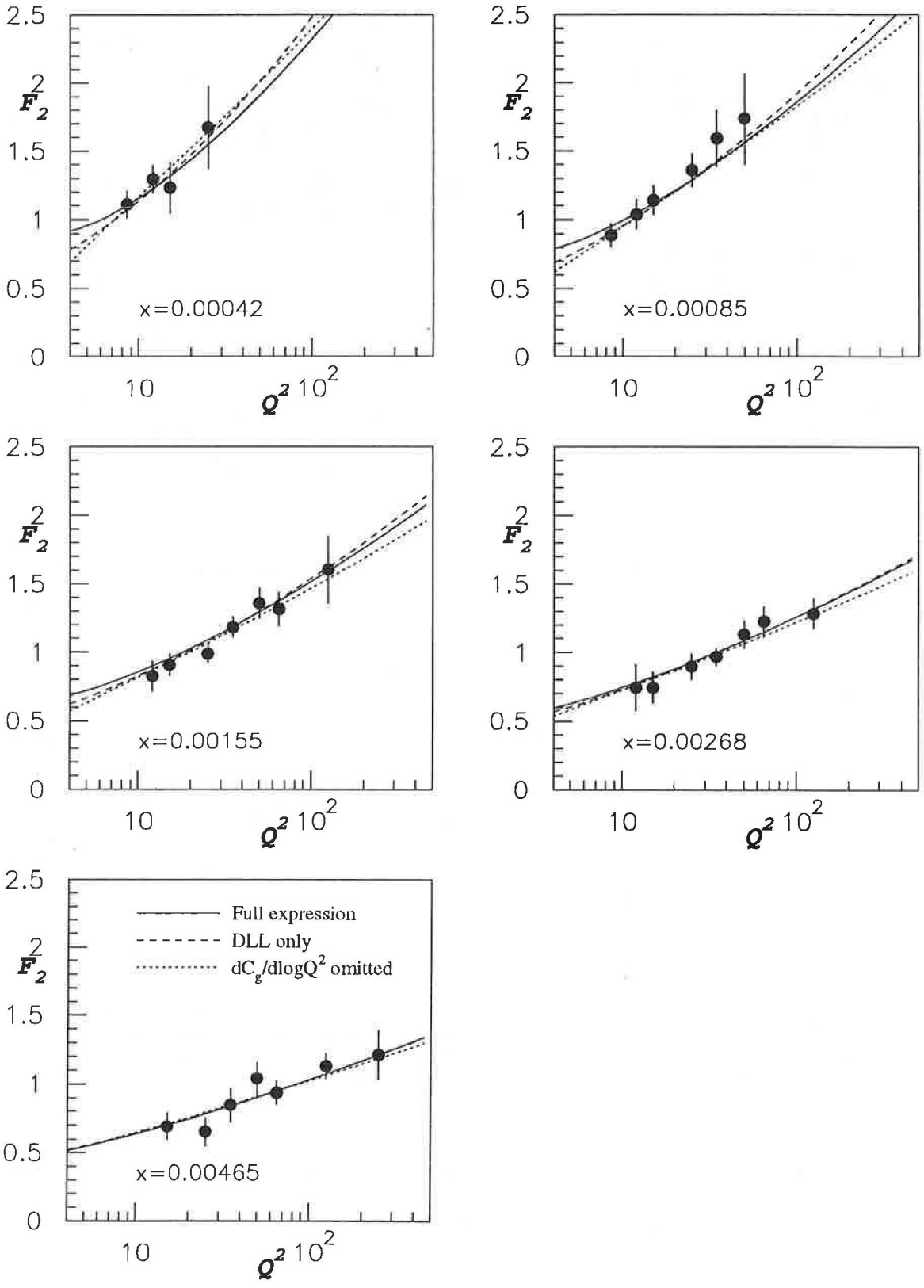

Fig. 4(b)